

Induction of tier-2 neutralizing antibodies in mice with a DNA-encoded HIV envelope native like trimer

Ziyang Xu^{1,2#}, Susanne Walker^{1#}, Megan C. Wise^{3#}, Neethu Chokkalingam^{1#}, Mansi Purwar^{1#}, Alan Moore^{4#}, Edgar Tello-Ruiz¹, Yuanhan Wu¹, Sonali Majumdar¹, Kylie M. Konrath^{1,2}, Abhijeet Kulkarni¹, Nicholas J Tursi^{1,2}, Faraz I. Zaidi¹, Emma L. Reuschel¹, Ishaan Patel¹, April Obeirne¹, Jianqiu Du⁴, Katherine Schultheis³, Lauren Gites³, Trevor Smith³, Janess Mendoza³, Kate E. Broderick³, Laurent Humeau³, Jesper Pallesen⁴, David B. Weiner¹, Daniel W. Kulp^{1*}

¹ Vaccine and Immunotherapy Center, The Wistar Institute, Philadelphia, PA 19104

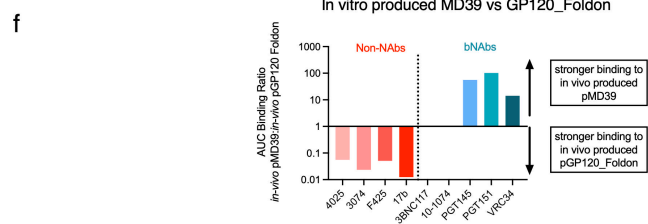
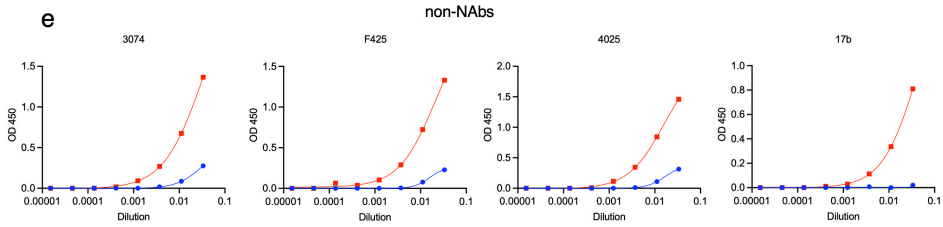
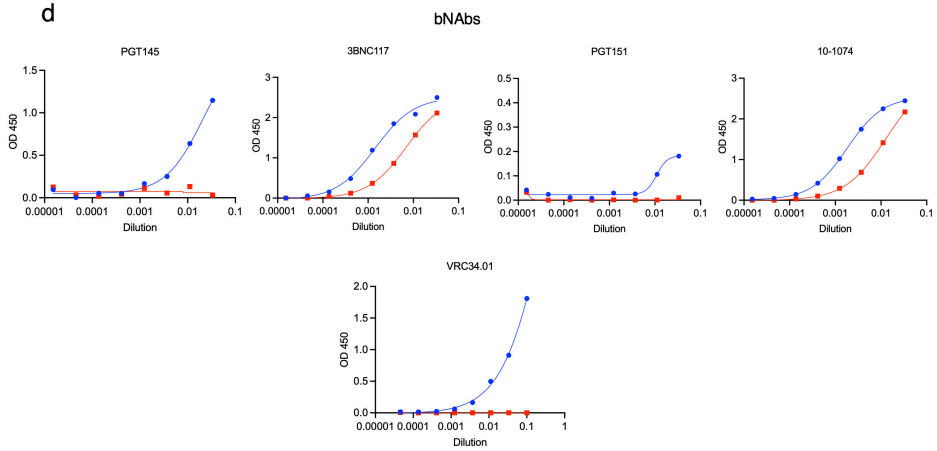
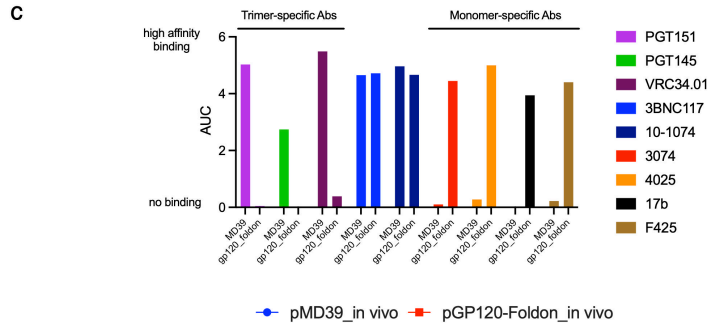
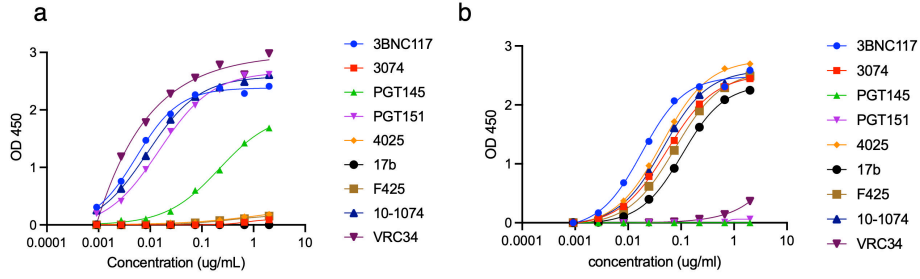
² Perelman School of Medicine, University of Pennsylvania, Philadelphia, PA 19104.

³ Inovio Pharmaceuticals, Plymouth Meeting, PA, 19462

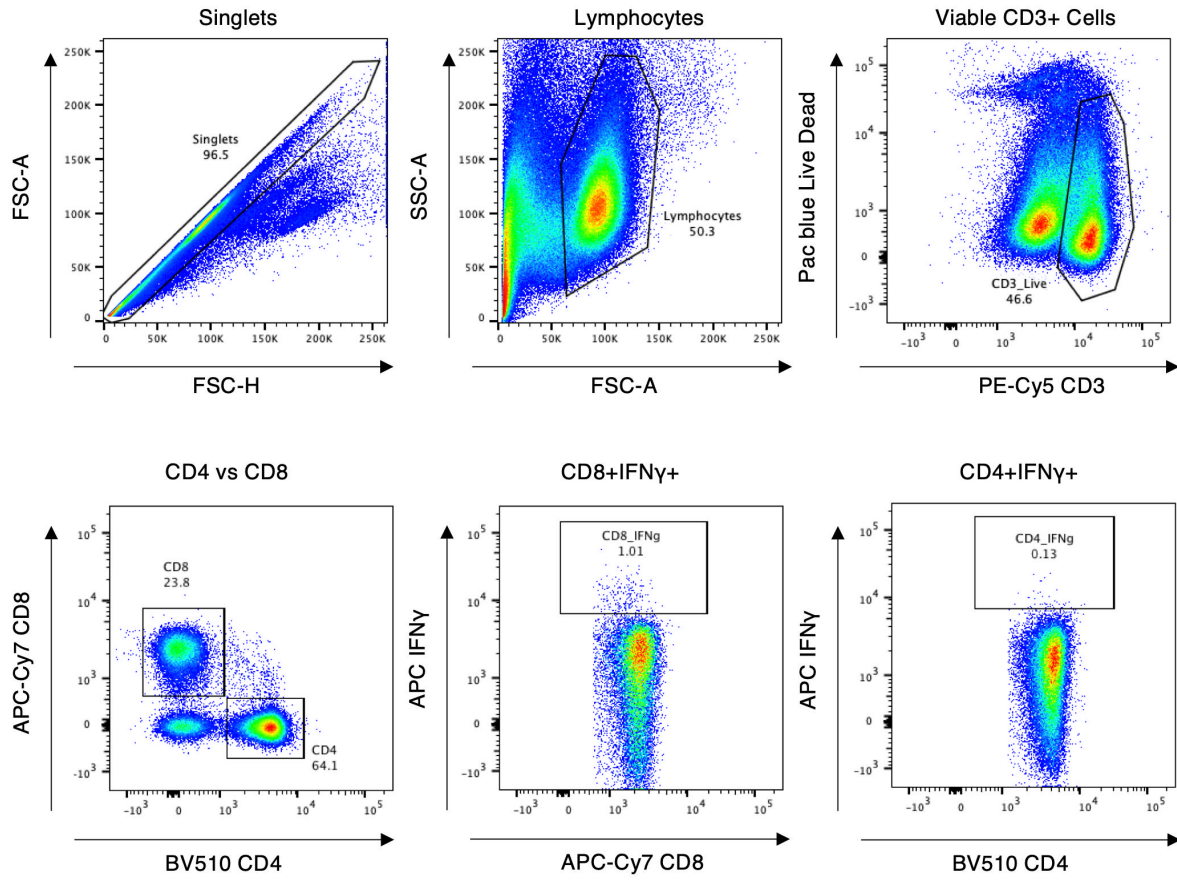
⁴ Molecular and Cellular Biochemistry, Indiana University, Bloomington, IN, 47405

*Corresponding Author: dwkulp@wistar.org

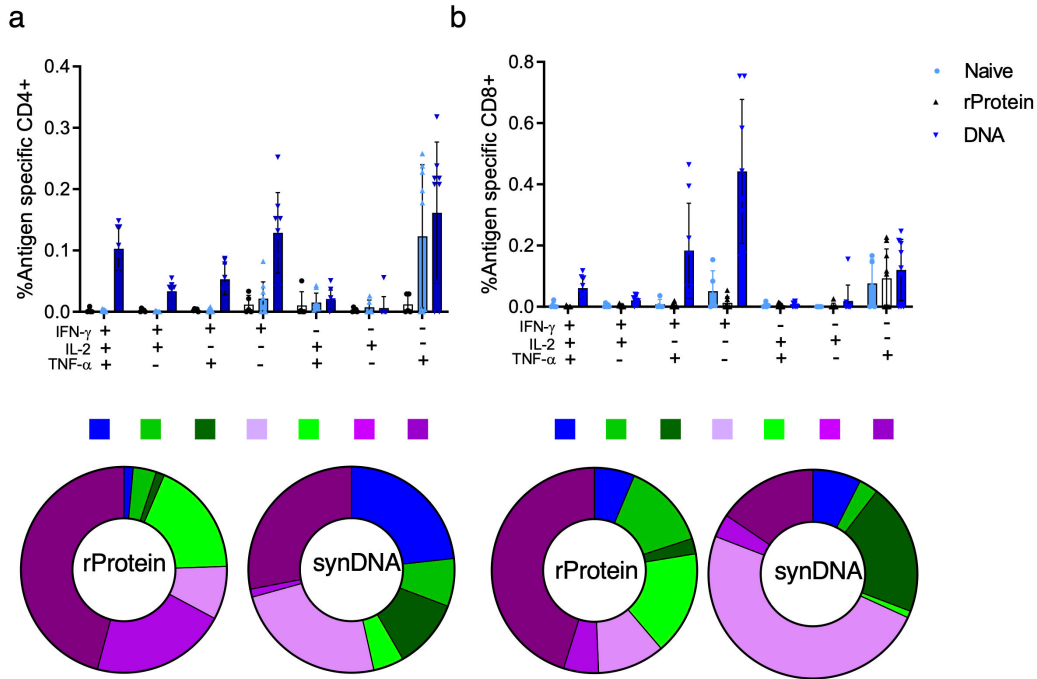
#These authors contributed equally to this work



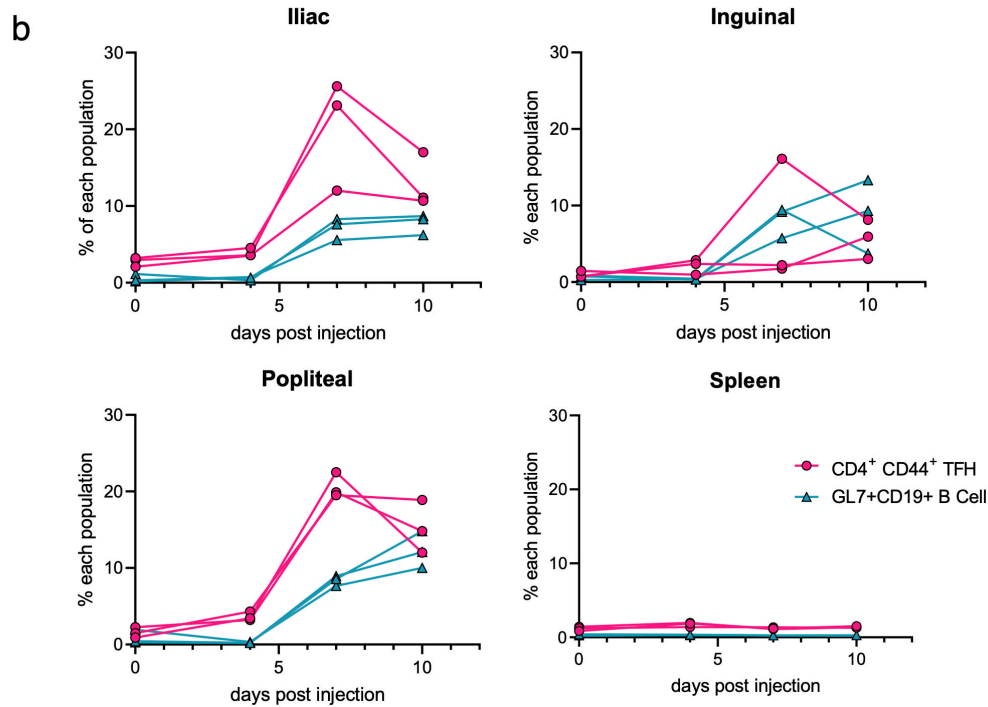
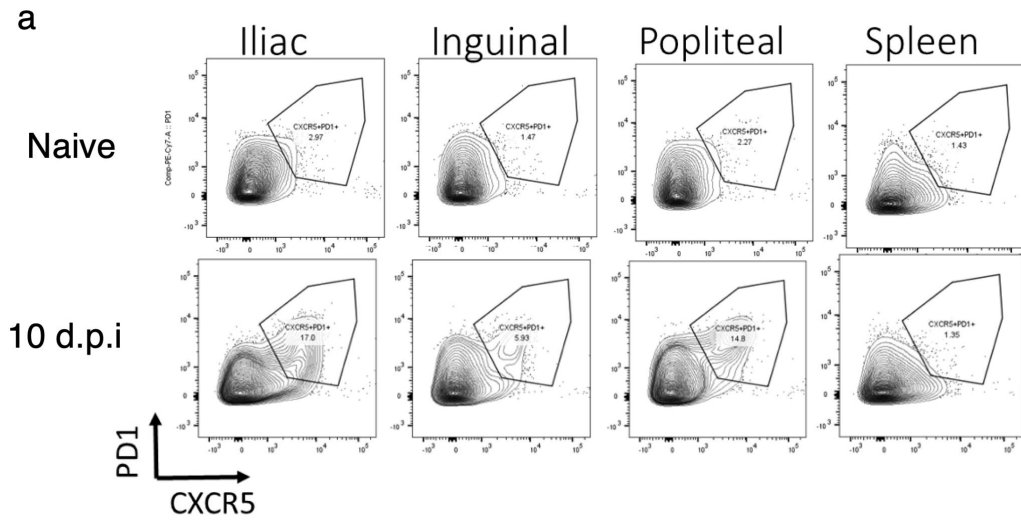
Supplementary Figure 1. Full antigenic profile of *in vitro* expressed MD39 vs BG505.gp120_foldon (related to Figure 1). (A) Binding of MD39 to HIV bNAbs PGT145, PGT151, VRC34.01, 3BNC117, 10-1074 or non-NAbs F425, 3074, 4025, 17B. (B) Binding of BG505.gp120_foldon to HIV bNAbs and non-NAbs as in (A). (C) Quantification of binding of MD39 or BG505.gp120_foldon to HIV bNAbs or non-NAbs in terms of Area Under Curve (AUC). (D and E) Binding of *in vivo* produced MD39 (blue) and GP120-foldon (red) to bNAbs PGT145, 3BNC117, PGT151, 10-1074 and VRC34.01 (D) and non-NAbs 3074, F425, 4025 and 17b (E). (F) Normalized area under the curve (ratio of *in vitro* produced pMD39 binding versus pGP120-foldon binding) for binding to HIV bNAbs and non-NAbs.



Supplementary Figure 2. ICS Gating scheme. Gating scheme used to determine cytokine positive CD4⁺ or CD8⁺ T cells following peptide stimulation (related to Figure 2 and 3).

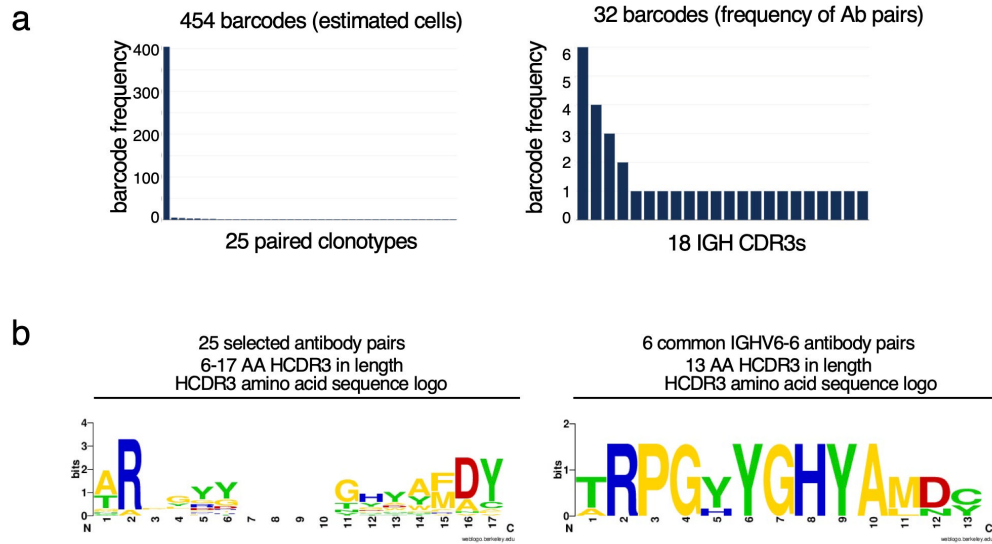


Supplementary Figure 3. DNA-encoded BG505.MD39 but not protein BG505.MD39 induced polyfunctional T-cell responses in BALB/c mice (related to Figure 2). Mice were immunized with 25ug of either DNA-encoded BG505.MD39 or RIBI-co-formulated protein BG505.MD39 at weeks 0, 3, 6 and euthanized at week 8 for cellular analysis. **(A – B)** ICS analyses of co-expression of IFN γ , TNF α and IL-2 cytokines in CD4⁺ **(A)** or CD8⁺ **(B)** T cells following stimulation with BG505 Envelope specific peptide pools. Two independent experiments were performed for each panel in the figure with similar findings. N=10 mice/group. Error bar represents standard deviation. Center of the error bar represents the mean. Source data are provided as a Source Data file.

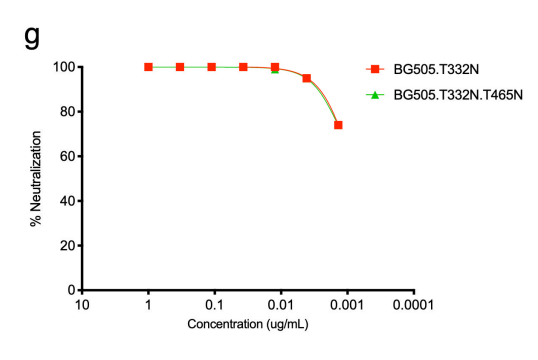
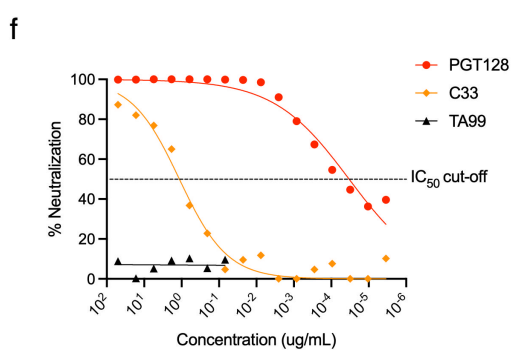
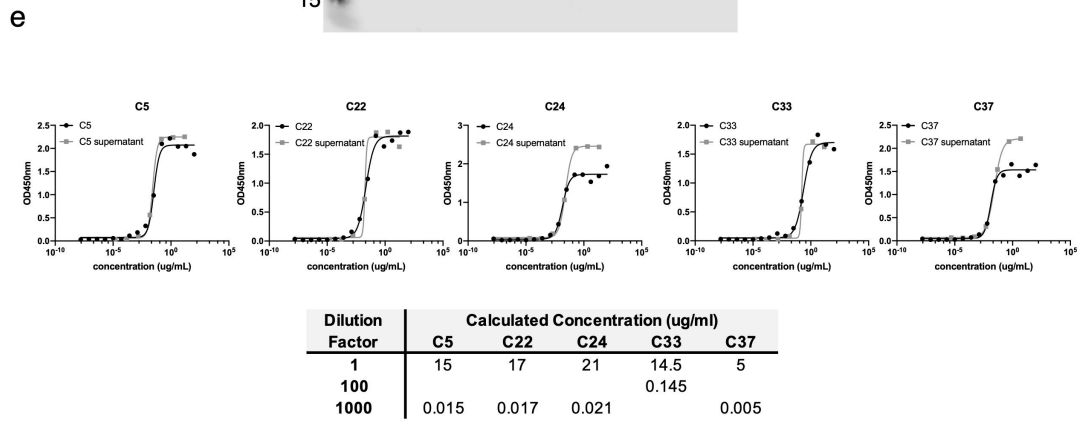
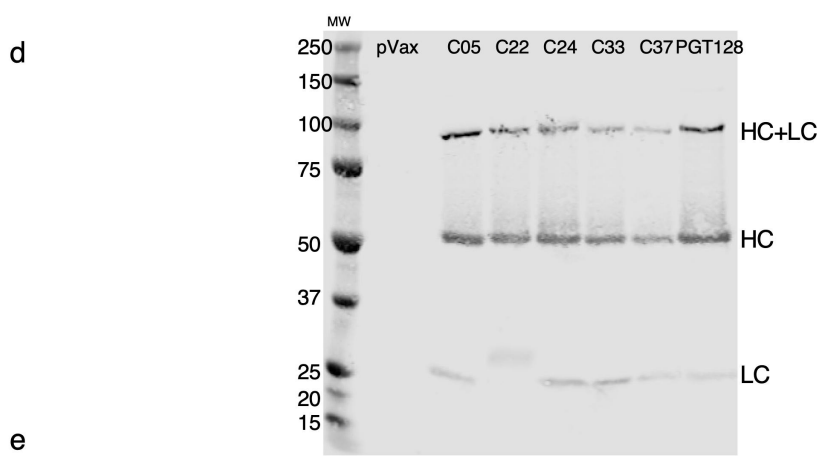
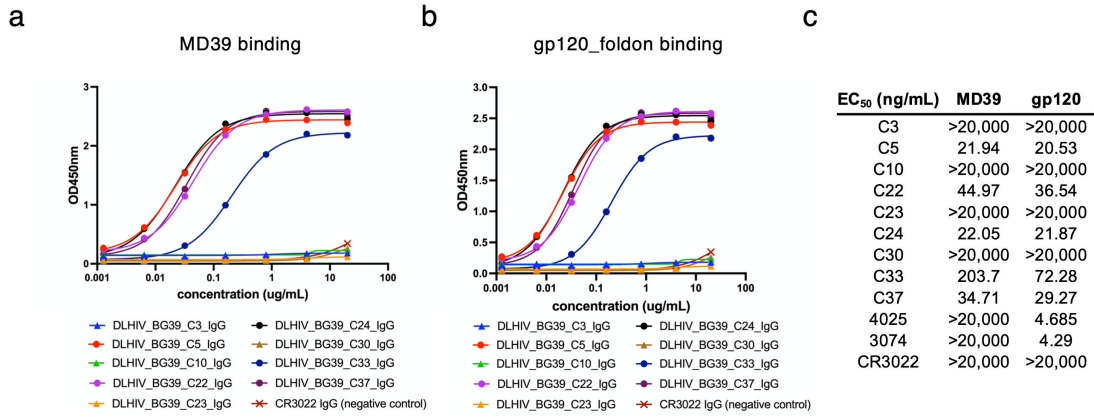


Supplementary Figure 4. DNA-encoded BG505.MD39 vaccination induced both Tfh and GC B cell responses in BALB/c mice (related to Figure 2). Mice were immunized with 25ug of DNA-encoded BG505.MD39 on Day 0 and euthanized sequentially on Days 4, 7 and 10 for analyses of Tfh and GC B cells. **(A)** Comparison of flow plots of CXCR5+PD1+ cells amongst CD4+CD44+ cells in the iliac, inguinal, popliteal and spleen of naive mice versus mice immunized with DNA-encoded BG505.MD39 10 d.p.i. **(B)** Kinetics of Tfh and GC B cell responses in the draining lymph nodes or spleens of mice vaccinated with DNA-encoded

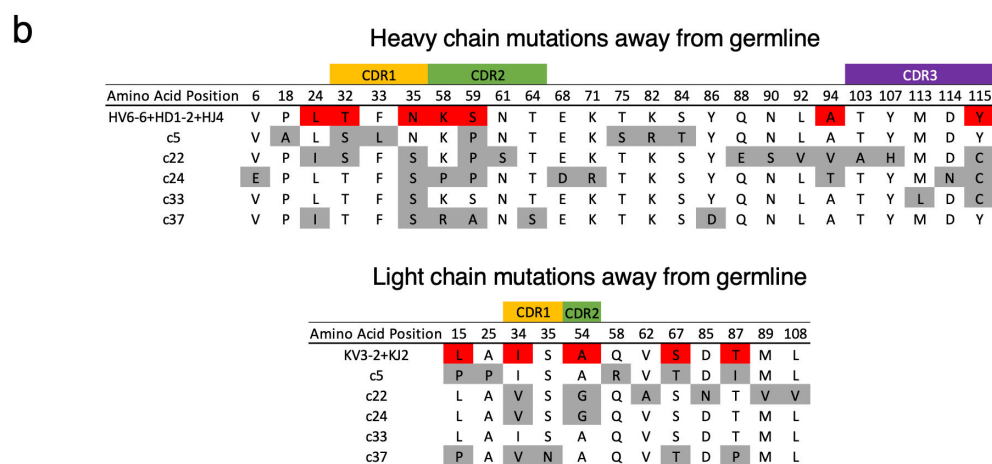
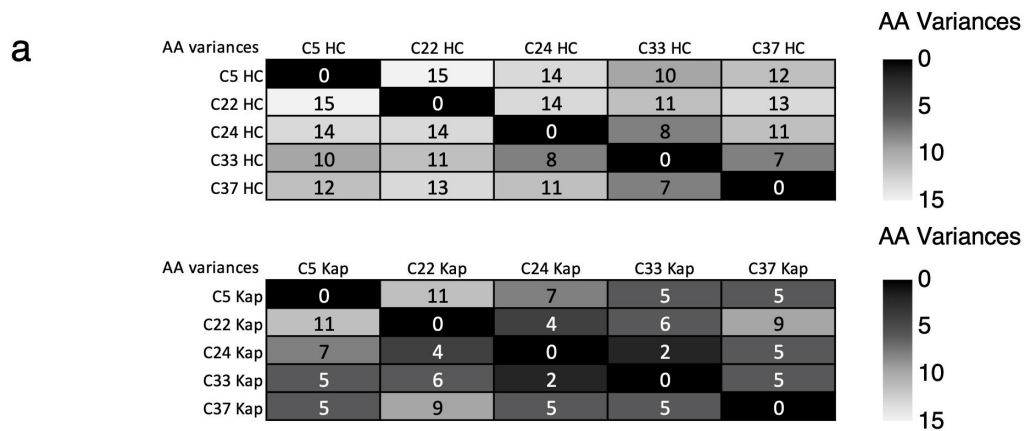
BG505.MD39. One independent experiment was performed for each panel in the figure. Each line represents an animal. N=3 mice/group. Source data are provided as a Source Data file.



Supplementary Figure 6. Sequence features of recovered murine antibody clones (related to Figure 5). (A) Demonstration of the barcode frequencies by clones (Left) or IGH HCDR3 identities (Right). (B) HCDR3 features of the 25 recovered MAb clones (left) or the 6 clones with IGHV6-6 germline VH gene usage (Right).

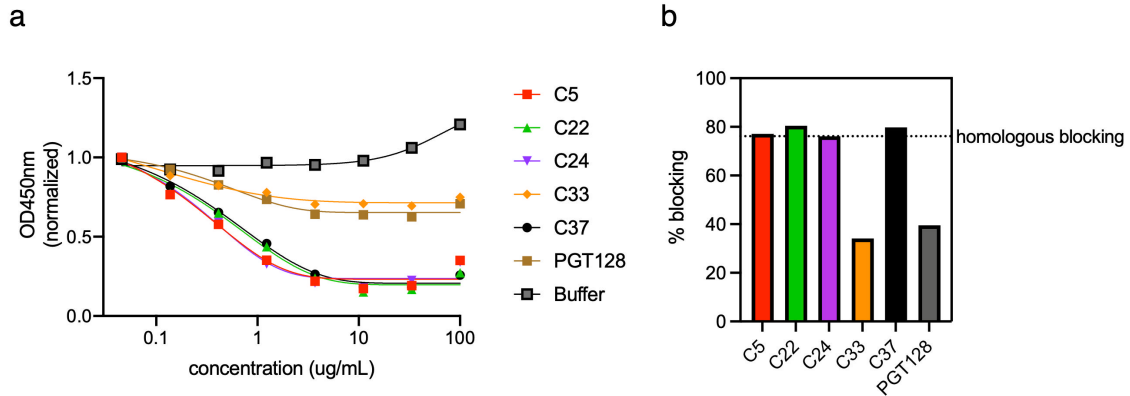


Supplementary Figure 7. Further characterizations of BG505.MD39-specific murine antibody clones (related to Figure 6). (A-C) Binding of all isolated murine mAb clones to BG505.MD39 (A) or gp120_foldon (B) as determined by ELISA, and respective measured EC₅₀ values (C). (D) Reducing SDS PAGE analysis of BG505.MD39-specific MAb clones C05, C22, C24, C33, and C37 in comparison with PGT128 or backbone pVAX vector transfection supernatants. (E) Determination of the antibody concentrations from the transfection supernatants based on BG505.MD39 binding in comparison with purified protein standards. (F) Neutralization of autologous BG505.T332N virus by PGT128 (positive control), C33, and murine IgG2A antibody TA99 (negative control) starting at 50ug/mL. (G) Comparison of neutralization potential of PGT128 with BG505.T332N pseudo-virus versus BG505.T332N.T465N pseudo-virus. For (D), the experiments were repeated twice.

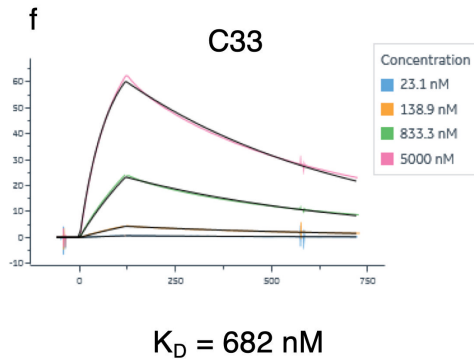
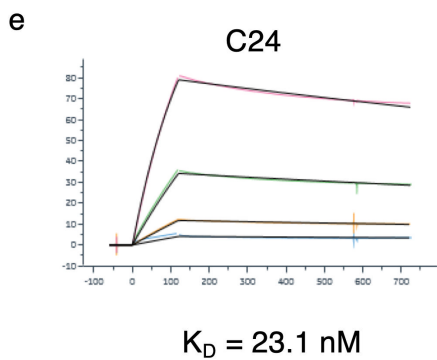
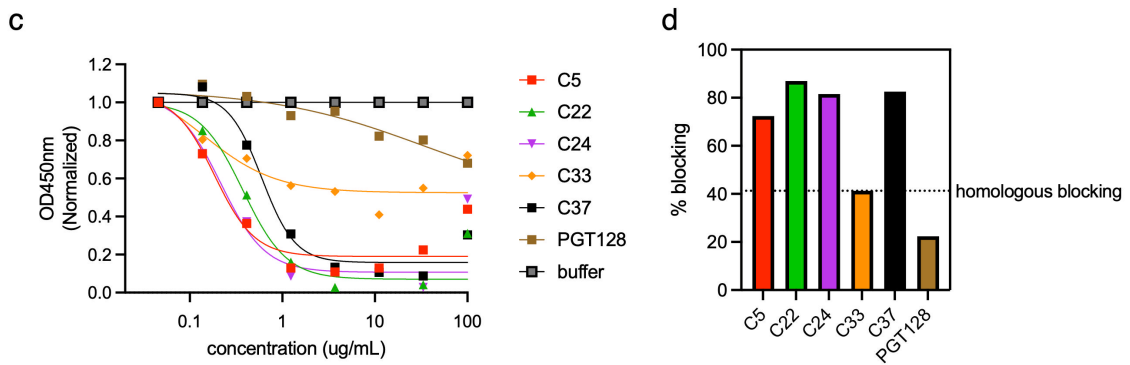


Supplementary Figure 8. Additional sequence features of recovered murine antibody clones (related to Figure 6). Comparisons of the heavy and light chain sequences of the 5 BG505.MD39-specific MAb clones by number of mutations (A) and positions for the mutations (B).

C24 Competition ELISA



C33 Competition ELISA



Supplementary Figure 9. Assessment of epitope specificity and affinities of C24 and C33 by competition ELISA and SPR (related to Figure 6). (A) Degree of binding of biotinylated C24 to MD39 in the presence of varying concentrations of non-biotinylated C05, C22, C24, C33, C37 and control buffer. (B) Degree of blocking of biotinylated C24 binding to MD39 by each of the aforementioned antibodies, as calculated

from (A). (C) Degree of binding of biotinylated C33 to MD39 in the presence of varying concentrations of non-biotinylated C05, C22, C24, C33, C37 and control buffer. (D) Degree of blocking of biotinylated C33 binding to MD39 by each of the aforementioned antibodies, as calculated from (C). (E and F) SPR trace to determine the binding and dissociation pattern of C24 (E) and C33 (F) to GP120 (to preserve 1:1 binding ratio). For (A-D), two technical replicates were determined for each experimental condition; error bar represents standard deviation. Source data are provided as a Source Data file.

Cryo-EM data processing

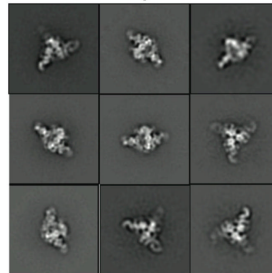
6150 movie micrographs

↓
frame motion correction, spectral weighting and summation



↓
reference-free LoG picking

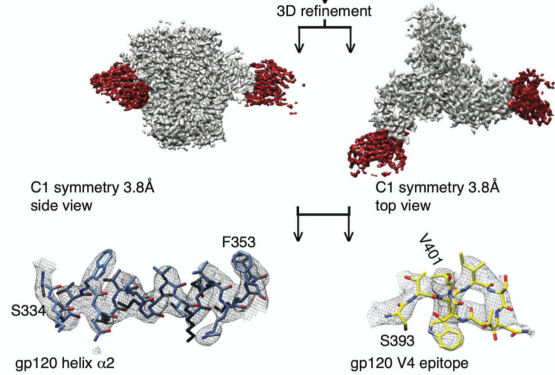
↓
reference-free 2D classification



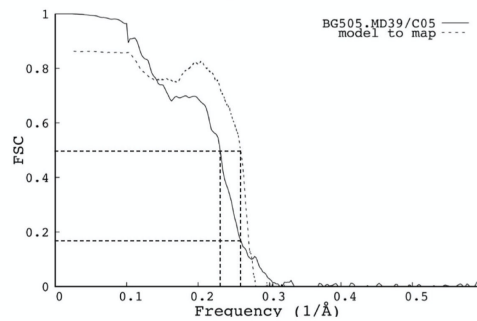
↓
manual inspection

↓
121,929 molecular projection images

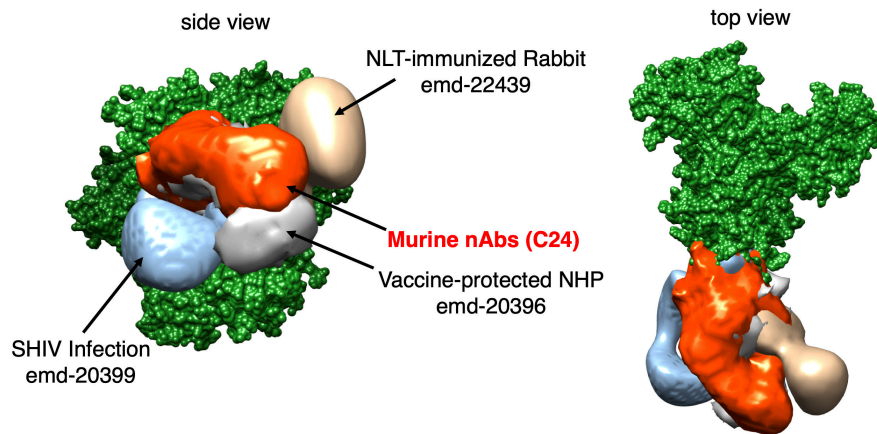
↓
3D refinement



FSC curve



Supplementary Figure 10. Cryo-EM data processing flow diagram resulting in a density map at 3.8Å global resolution (FSC 0.143 consistency between two independently refined data half sets) (related to Figure 7). Flow diagram comprises panels of representative map densities with corresponding atomic models superimposed as well as a standard Fourier shell correlation plot (FSC plot). MD39 is shown in grey; C05 Fab is shown in dark red.



Supplementary Figure 11. Computational modeling of murine mAbs bound to NLT. Comparison of the angle of approach in terms of binding to NLT between murine and NHP V5-directed mAbs (**related to Figure 7**).

Supplementary Table 1. Comparison of neutralizing antibody titers in mice immunized with DNA-encoded NLT versus protein MD39. BG505.T332N or MLV ID50 neutralization titers in the sera of animals immunized with 25ug RIBI co-formulated protein BG505.MD39 or DNA-encoded BG505.MD39 at Weeks 0, 3, 6 two weeks post the final vaccination.

	Mouse ID	BG505.T332N	MLV
Protein	1	<45	<45
	2	<45	<45
	3	<45	<45
	4	<45	<45
	5	<45	<45
	6	<45	<45
	7	<45	<45
	8	<45	<45
	9	<45	<45
	10	<45	<45
DNA	1	<45	<45
	2	<45	<45
	3	232	<45
	4	<45	<45
	5	<45	<45
	6	73	<45
	7	50	<45
	8	<45	<45
	9	<45	<45
	10	<45	<45

Supplementary Table 2. Comparison of neutralizing antibody titers in mice immunized with DNA-encoded NLT using a short versus a long boost scheme. BG505.T332N or MLV ID50 neutralization titers in the sera of naïve mice or animals immunized with 25ug DNA-encoded BG505.MD39 at Weeks 0, 3, 6 (short scheme) or Weeks 0, 3, 16 (long scheme) two weeks post the final vaccination.

	Mouse ID	BG505.T332N	MLV
Naïve	1	<45	<45
	2	<45	<45
	3	<45	<45
	4	<45	<45
	5	<45	<45
Short	1	<45	<45
	2	<45	<45
	3	<45	<45
	4	>1215	<45
	5	83	<45
	6	132	<45
	7	<45	<45
	8	<45	<45
	9	<45	<45
	10	<45	<45
Long	1	>1215	<45
	2	48	<45
	3	>1215	<45
	4	824	<45
	5	<45	<45
	6	194	<45
	7	53	<45
	8	<45	<45
	9	46	<45
	10	<45	<45

Supplementary Table 3. Key statistics of cryo-EM data processing, model building and validation.

Map	BG505.MD39TS/C05
PDB code	7SQ1
EMDB code	25376
Data collection	
Microscope	FEI Titan Krios
Voltage (kV)	300
Detector	Gatan K3
Recording mode	Counting
Magnification (incl. post-magnification; EFTEM)	105,000
Movie micrograph pixelsize (Å)	0.84
Dose rate (e ⁻ /[(camera pixel)*s])	16.372
Number of frames per movie micrograph	60
Frame exposure time (ms)	50
Movie micrograph exposure time (s)	2.59
Total dose (e ⁻ /Å ²)	60.6
Defocus range (µm)	0.4-3.3
EM data processing	
Number of movie micrographs	5,485
Number of molecular projection images in map	121,929
Symmetry	C1
Map resolution (FSC 0.143; Å)	3.8
Map sharpening B-factor (Å ²)	-75
Structure Building and Validation	
Number of atoms in deposited model	18,364
gp120	3,962
gp41	1,025
glycans	1,373
MolProbity score	1.147 (99%)
Clashscore	3.57
EMRinger score	2.37
model to map correlation (FSC 0.5; Å)	3.8
Deviations from ideal	
Bond length outliers (RMSD; Å, #)	0.011 (0)
Bond angles outliers (RMSD; °, #)	1.499 (28)
Ramachandran plot	
Favored (%)	98.77
Allowed (%)	1.18
Outliers (%)	0.04

Supplementary Note 1

Nucleic acid sequence: C05_HC_VH

GAAGTGAAGCTTGAGGAGTCTGGAGGAGGCTTGGTGCAAGCTGGAGGATCCATGAAACTCTCCTGTGTTGCCTCT
GGATTCAGTCTCAGTAATTATTGGATGAACTGGGTCCGCCAGTCTCCAGAGAAGGGGCTTGAGTGGGTTGCTGAA
ATTAGATTGAAGCCTCAAAATTATGCAACACATTATGCGGAGTCTGTGAAAGGGAGGTTTCAGCATCTCAAGAGAT
GATTCAGAAGTACTGTCTACCTGCAAATGAACAACCTTAAGAGCTGAAGACACTGGCATTATTACTGTACCAGGC
CGGGATACTACGGCCACTATGCTATGGACTACTGGGGTCAAGGAACCTCAGTCACCGTCTCCTCA

Nucleic acid sequence: C05_Kappa

GACATTGTGCTGACCCAGTCTCCAGCTTCTTTGGCTGTGTCTCCAGGTCAGAGGGCCACCATCTCCTGCAGACCCA
GCGAAAGTGTGATAATTACGGCATTAGCTTTATGAACTGGTTCCAACAGAAACCAGGACAGCCACCCAAACTCCT
CATCTATGCTGCATCCAACCGAGGATCCGGGGTCCCTGCCAGGTTTACTGGCAGTGGGTCTGGGACAGACTTCAG
CCTCAACATCCATCCTATGGAGGAGGATGATATTGCAATGTATTTCTGTCAGCAAAGTAAGGAGGTTCCGTATACG
TTCGGAGGGGGGACCAAACCTGGAAATAAAA